Effect of region-dependent viscoelastic properties on the TMJ articular disc relaxation under prolonged clenching.

Natalia García[a], Pelayo Fernández[a,*], Eiji Tanaka[b], Eva Barrientos[a], María Jesús Lamela-Rey[a], Alfonso Fernández-Canteli[a], Juan Carlos de Vicente[c]

[a] Department of Construction and Manufacturing Engineering, University of Oviedo, Gijón, Spain
[b] Department of Orthodontics and Dentofacial Orthopedics, Institute of Biomedical Sciences, Tokushima University Graduate School, Tokushima Japan
[c] Department of Surgery and Medical Surgical Specialities, University of Oviedo, Oviedo, Spain

*Corresponding author:
Pelayo Fernández
Department of Construction and Manufacturing Engineering
University of Oviedo, Gijon, España (Spain)
E-mail: fernandezpelayo@uniovi.es

Keywords

Clenching, TMJ, viscoelastic behavior, stress analysis, material model

Abstract

The disc of the temporomandibular joint (TMJ) is located between the mandibular condyle and temporal bone, and has an important load-bearing and stress absorbing function. The TMJ disc presents viscoelastic characteristics that are largely dependent on its collagen fibre and proteoglycan composition and organization. The purpose of this study is to investigate the possible effects of region-specific dynamic viscoelastic properties on stress relaxation during prolonged clenching.

Two finite element models were used to compare the stress distribution within the TMJ disc, namely, one with uniform disc material property and another one with region-specific disc material properties. Similar results were observed in both models with slight differences in the location of maximum stress. Larger stresses were observed in all cases for the model with uniform disc material property. Moreover, the higher values for the model with uniform disc material property appeared in the lateral region, while in the model with region-specific disc

properties, these values moved to the lateral and central region.

This investigation confirms that both models are sufficiently accurate to investigate stress distribution in the TMJ disc, and, particularly, the model with the region-specific disc material properties ensure better simulations of the TMJ disc behaviour.

1 Introduction

The disc of the temporomandibular joint (TMJ) is located between the mandibular condyle and temporal bone and has an important load-bearing, stress absorbing and joint stabilizing function during various mandibular movements working also as articular cartilage (Barrientos et al., 2016, 2020; Fernández et al., 2013; Tanaka et al., 2008; Eiji Tanaka & van Eijden, 2003). As sliding and rotating with slightly lateral excursion occur simultaneously between articulating surfaces, the TMJ disc is subjected to a multitude of different loading modes, according to the region, and undergoes a deformation commensurate with its material properties (Tanaka & van Eijden, 2003).

Like other articular cartilages, the TMJ disc exhibits not only elastic but also viscous characteristics. The viscoelastic properties are mainly the result of fluid flow into and out of the disc (Detamore & Athanasiou, 2003; Tanaka & van Eijden, 2003). The disc contains variable amounts of cells and an extracellular matrix including macromolecules and fluid. These macromolecules consist mainly of collagen (85-90%) and proteoglycans (10-15%) (Nakano and Scott, 1989; Sindelar et al., 2000). The viscoelastic properties of the disc are largely dependent on its collagen fibre and proteoglycan composition and distribution and on their interaction with the tissue fluid (Detamore et al., 2005; Scapino et al., 1996). It is also acknowledged that there are regional contrasts among the distribution of collagen fibres and proteoglycans in the TMJ disc (Detamore et al., 2005; Mizoguchi et al., 1998; Tanaka and van Eijden, 2003). This configuration might allow the TMJ components to withstand the complicated compressive, tensile and shear stress distribution prevailing during its function (del Pozo et al., 2002).

Until now, numerous studies have been performed to determine the regional difference of the dynamic viscoelastic properties of the TMJ disc (Fernández et al., 2013; Tanaka et al., 2006). Fernández et al. (2013) indicates that the dynamic viscoelastic properties are region-specific and depend on the loading frequency, thus having important implications for the transmission of load to the TMJ. Furthermore, the regional difference of the dynamic viscoelastic properties of the TMJ disc might contribute to proper energy dissipation and stress absorption in the TMJ during stress relaxation (Detamore & Athanasiou, 2003; Hattori-Hara et al., 2014; Tanaka et al., 2014).

On the other hand, the information about the region-specific dynamic viscoelastic parameters often makes difficult to fit a reasonable mechanical material model of the disc that could be used for further calculation on the TMJ, such as numerical models constructed with the finite element method. In this line, for previous studies of TMJ stress analyses, only one set of viscoelastic parameters has been commonly used for the TMJ disc (Abe et al., 2013; Barrientos et al., 2020; Donzelli et al., 2004; Hattori-Hara et al., 2014; Hirose et al., 2006; Koolstra & van Eijden, 2005; Pérez del Palomar & Doblaré, 2006; Tanaka et al., 2004), and no study has been reported in which the region-specific material properties of the TMJ disc were adopted to stress analyses with a finite element model of the TMJ. The purpose of this study was to investigate the possible effects of region-specific dynamic viscoelastic properties of the TMJ disc on stress relaxation during prolonged clenching. A finite element model of the TMJ based on magnetic resonance (MR) images from one healthy subject was constructed, and the distributions of stresses in the TMJ disc during prolonged clenching in different loading direction were analysed using a finite element model of the TMJ with the dynamic compressive properties in the five different regions of the TMJ disc. After that, a comparison between the behaviour of the disc using uniform material property and the region-dependent disc properties was performed.

2 Materials and Methods

The current investigation involved the development of a finite element model (FEM) in ABAQUS (Simulia, Dassault Systemes), in which the mechanical viscoelastic properties of the different regions of the TMJ disc were implemented. According to Fernández et al. (2013), five regions were selected and the region-specific relaxation moduli were obtained. This modelling allowed the analysis of the effects of region-specific viscoelastic properties of the TMJ disc on stress relaxation during prolonged clenching.

2.1 Materials

To obtain the region-specific mechanical properties of the disc, experimental data from Fernández et al. (2013) was collected. In order to obtain the relaxation moduli of the five regions, the Ninomiya-Ferry algorithm (Ninomiya and Ferry, 1959) was applied using MATLAB. Although a wide variety of methods can be used to performed the conversion between time-domain and frequency-domain, Ninomiya-Ferry was selected due to the good balance that it presents between the accurate results and the low calculus capacity needed (Emri et al., 2005). The region-specific relaxation moduli are presented in Figure 1 and the numerical values are given in appendix A: (Tables A1-A5).

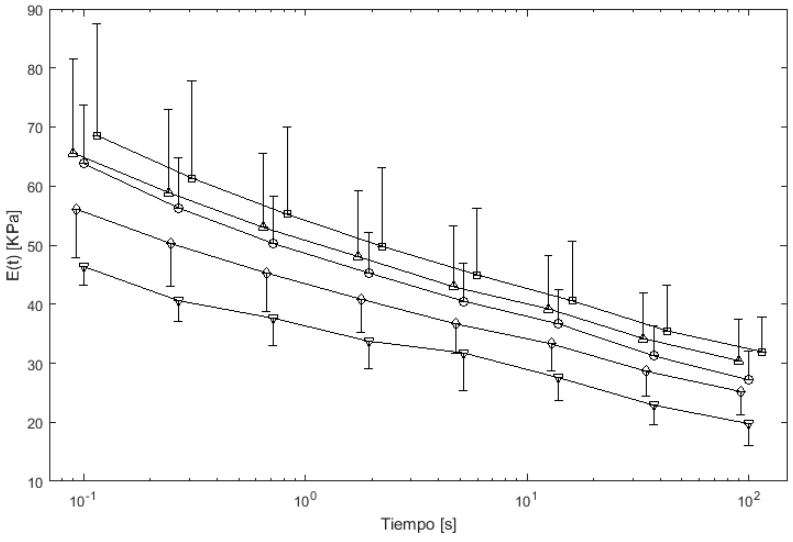

Figure 1. Relaxation modulus for each region: Posterior (□), Anterior (Δ), Central (○), Medial (◊) and Lateral (∇).

In order to use the region-specific relaxation moduli $E(t)$ in FEM, the curves were

fitted using the linear viscoelastic generalized Maxwell model (Chen, 2000; Tschoegl, 2012).

$$E(t) = E_0 \left[1 - \sum_{i=1}^{n_t} e_i \left(1 - exp\left(-\frac{t}{\tau_i}\right)\right)\right] \quad (1)$$

where τ_i are the times, e_i the modulus ratios and E_0 is the instantaneous modulus. The material model was fitted using an optimized Prony series method (Barrientos et al., 2019). This method optimizes the best locations for both times (τ_i) and modulus ratios (e_i) in order to minimize the number of prony terms necessary in the material model. For the present relaxation curves (see Figure 1) and based on the numerical errors in the fittings for the homgenous and optimal discrete time distributions (Barrientos et al., 2019), the optimized model is obtained when 3 prony series terms are used being the error 0.04%. The viscoelastic models (see Eq. (1)) fitted for each region are presented in appendix A (Tables A6-A10).

2.2 Finite element model

To examine the stress relaxation during prolonged clenching in the TMJ disc, a finite element model of the TMJ, based on Barrientos et al. (2020), was implemented in ABAQUS (Simulia, Dassault Systemes).

In order to introduce the region-specific mechanical material properties, the disc from Barrientos et al. (2020), modelled as 3D deformable solid, had to be modified. On the other hand, temporal bone and cartilages were modelled as discrete rigid solids (Barrientos et al., 2020). Finally, both condylar and temporal cartilages were modelled using skin shell elements with linear elastic properties (see Table 1).

Table 1. Material properties for the cartilages (from Tanaka et al., 2014)

Model part	Young Modulus, E [MPa]	Poisson ratio, ν
Condylar cartilage	0.8	0.3
Temporal cartilage	1.5	0.3

As a first step, the geometry of the disc was split into five regions: anterior (A), posterior (P), Lateral (L), Medial (M) and Central (C). The regional division,

showed in Figure 2, was assumed in agreement with the experimental methodology used to obtain the dynamic viscoelastic parameters (Fernández et al., 2013), with the morphology of the articular disc and with the viability of the modelling procedure. Additionally, the viscoelastic material models previously obtained (section 2.1 Materials) were directly assigned to each corresponding region. Finally, a mesh sensitivity analysis was carried out and considering the convergence of the results and the computational costs, linear tetrahedral elements of approximately 0.5 mm size were chosen.

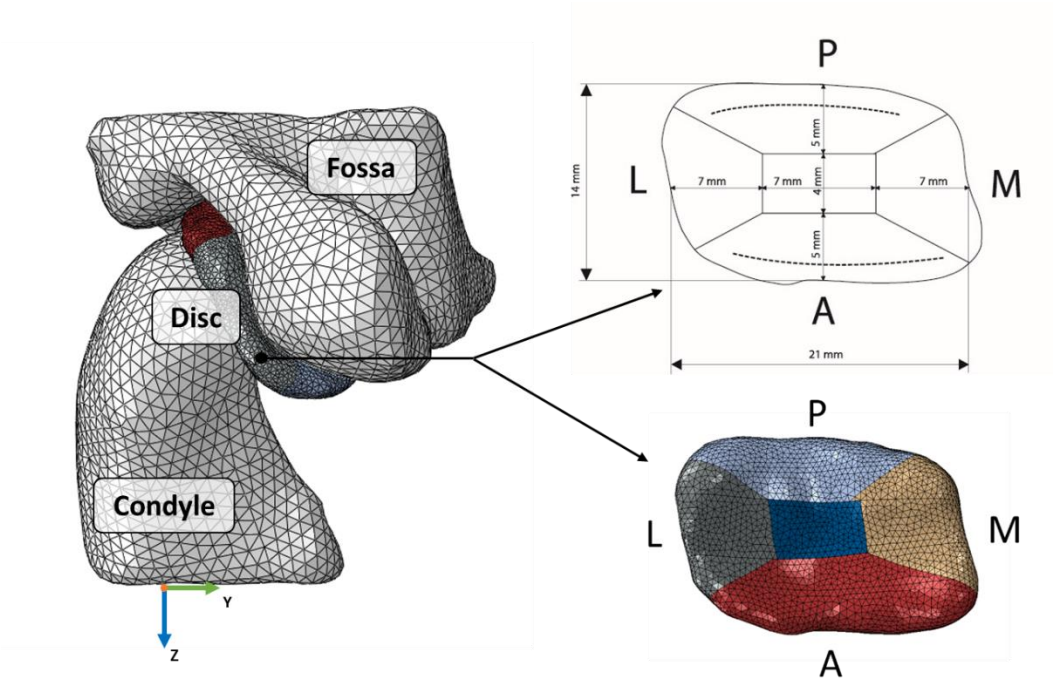

Figure 2. Regions created in the FE model for defining each material region.

In order to avoid the influence and uncertainties in the contacts between model parts, TIE contacts were used. In this type of contacts, nodes on the slave surface have the same value of displacement as the point on the master surface that it contacts. (Simulia, 2016)

Finally, the region-specific FEM was also used for comparison with the case of uniform disc material properties. With this aim, the same material was assigned for the five regions described previously. The material used for the uniform mechanical properties disc was retrieved from Barrientos et al. (2020). The Prony coefficients for the generalized Maxwell model (see Eq. (1)) are presented in Table 2.

Table 2. Mechanical properties used for the uniform disc case (Barrientos et al., 2020)

Poisson ratio, ν	0.4
Young Modulus, E_0 [MPa]	0.18
Prony terms	
e_1	0.5733
τ_1	0.0384
e_2	0.1223
τ_2	0.4925
e_3	0.0818
τ_3	6.3499
e_4	0.0926
τ_4	106.4815

2.3 Simulations

In regard to the boundary conditions, the movement of the temporal bone was restricted, while only displacement of the condyle was allowed to simulate the clenching conditions.

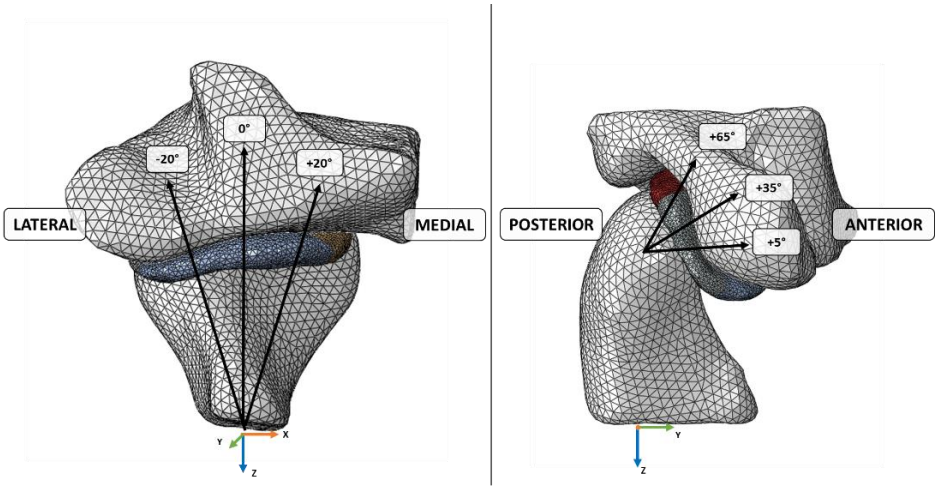

Figure 3. Illustration of the condylar directional loading applied in the simulation.

The loading conditions were defined taken into account the five regions considered in the disc (see Figure 2). For each define loading angle, the necessary displacements for applying a 10% compression strain in the disc were

estimated. The values for the displacements applied to the reference point of the condyle according to the model coordinate system (see Figure 3) in the medio-lateral direction are presented in Table 3.

Table 3. Loading angles used in the medio-lateral direction. (see Figure 3)

Angle	U_x [mm]	U_y [mm]	U_z [mm]
-20º	-0.035	0.096	-0.096
0º	0	0.1	-0.1
20º	0.035	0.096	-0.096

On the other hand, three loading angles as representative ranges of the TMJ movement were considered for the antero-posterior direction (see Table 4). These loading angles (see Figure 3) were selected according to the study of Beek et al. (2000).

Table 4. Loading angles used in the antero-posterior direction (see Figure 3).

Angle	U_x [mm]	U_y [mm]	U_z [mm]
65º	0	0.060	-0.128
35º	0	0.116	-0.081
5º	0	0.141	-0.012

The loading conditions applied and the simulation loading steps were exactly the same in both uniform properties and region-specific properties models. The simulations of prolonged clenching were made in different steps (Barrientos et al., 2020), described as the loading conditions illustrated in Figure 4.

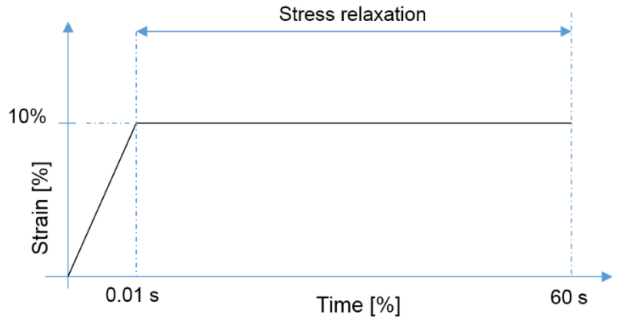

Figure 4. Loading conditions for simulation of prolonged clenching.

1

2

3. Results

In this study, the stress distribution on the TMJ disc of both models during prolonged clenching are shown at three different instances of time: t = 0.1 s, which corresponds to the first available data of the specific-region material ; t = 1 s, which represents an approximate relaxation ratio of about 50% in the material; and t = 60 s at the end of the relaxation step. Moreover, variations in the results due to the loading direction are studied.

3.1 Medio-lateral direction

Firstly, von Mises stress results of the both models in the medio-lateral direction are presented. The largest von Mises stresses on the surface of the TMJ disc due to medio-lateral loading variations were observed when the loading was applied at -20º direction. On the other hand, the lowest stresses were obtained when the loading direction was set to +20º as the stress distribution was more uniform.

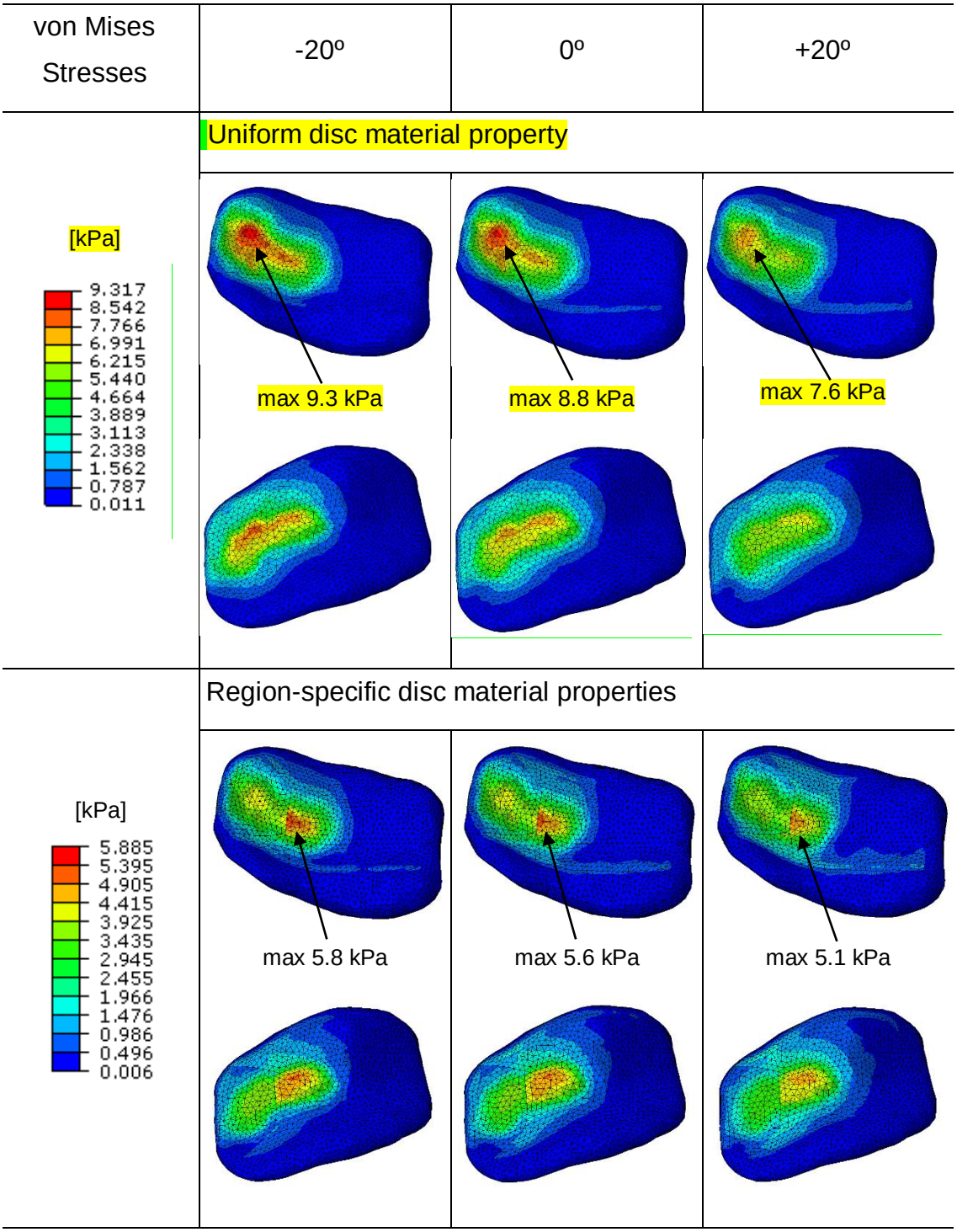

Figure 5. von Mises stresses in the disc at t = 0.1 s

In Figure 5, the largest von Mises stresses at t =0.1s were found in the model with uniform disc material property with a value of 9.3 kPa, whereas 5.8 kPa were obtained in the model with region-specific disc properties. This difference represents a reduction in stress of approximately 38% between models. On the other hand, as shown in Figure 6, the maximum stress values at t = 1 s were 6.3

kPa for the model with uniform disc property and 4.6 kPa for the model with region-specific disc properties, which represents a reduction in stress of approximately 28%. In addition, stresses after relaxation (t = 60 s) in both models are presented in Figure 7. Higher stress values are also obtained for the model with uniform disc property. The maximum stress values were 4.2 kPa for the model with uniform disc property and 2.9 kPa for the model with region-specific disc properties, which represents a reduction in stress of approximately 30% between models.

von Mises Stresses	-20º	0º	+20º
	Uniform disc material property		
[kPa] 6.874 6.302 5.729 5.157 4.585 4.012 3.440 2.868 2.295 1.723 1.151 0.578 0.006	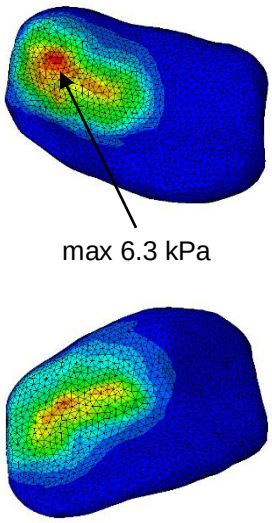	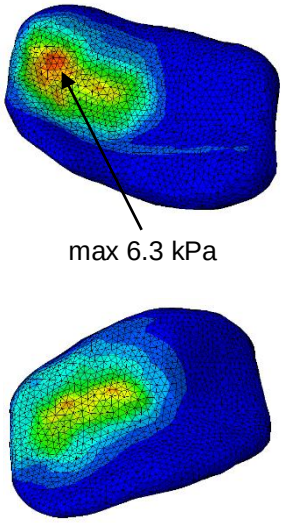	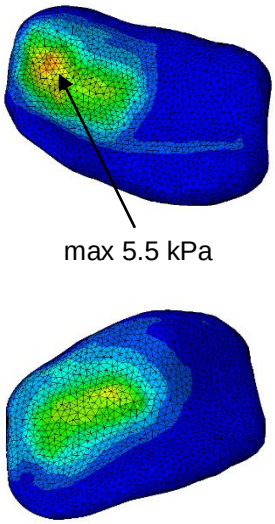
	Region-specific disc material properties		
[kPa] 4.629 4.243 3.858 3.473 3.088 2.703 2.317 1.932 1.547 1.162 0.776 0.391 0.006	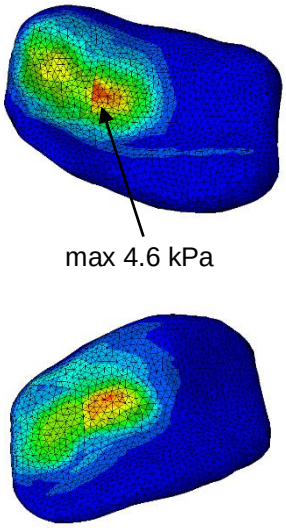	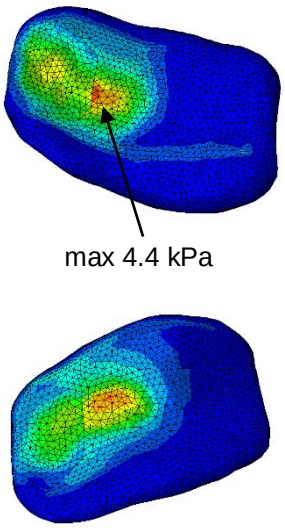	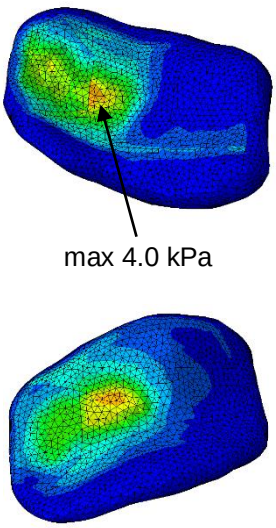

Figure 6. von Mises stresses in the disc at t = 1 s.

Concerning the location of the largest von Mises stresses, in the model with uniform disc property the largest von Mises stresses were located in the lateral region, while, in the model with region-specific disc properties, were also in the lateral region but closer to central region of the disc, both at t = 0.1 s and t = 60 s. (See Figures 5 and 7). However, at t = 1 s, as it can be seen in Figure 6, stress

distribution was similar to those previously commented with a slight increment in stress towards the anterior zone.

von Mises Stresses	-20º	0º	+20º
	Uniform disc material property		
[kPa] 4.356 3.994 3.631 3.268 2.906 2.543 2.180 1.817 1.455 1.092 0.729 0.367 0.004	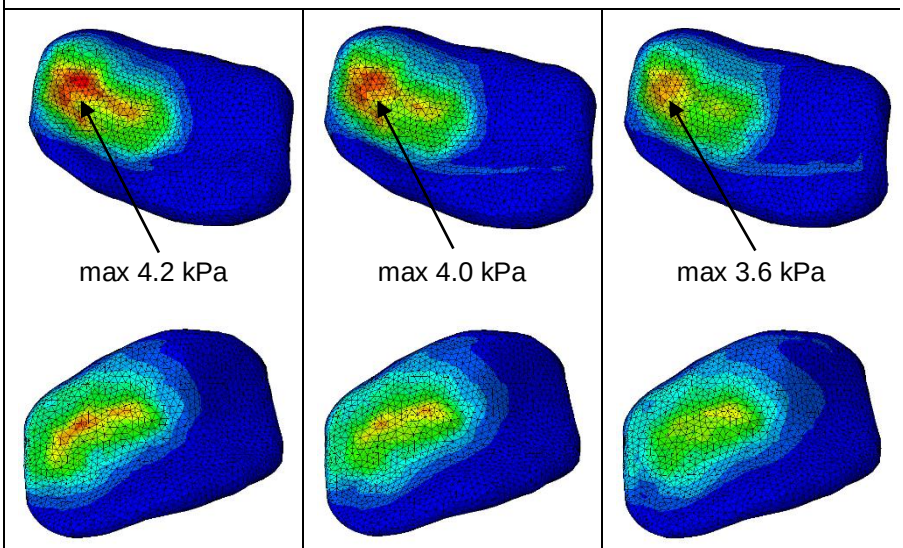		
	Region-specific disc material properties		
[kPa] 2.940 2.695 2.450 2.206 1.961 1.716 1.472 1.227 0.983 0.738 0.493 0.249 0.004	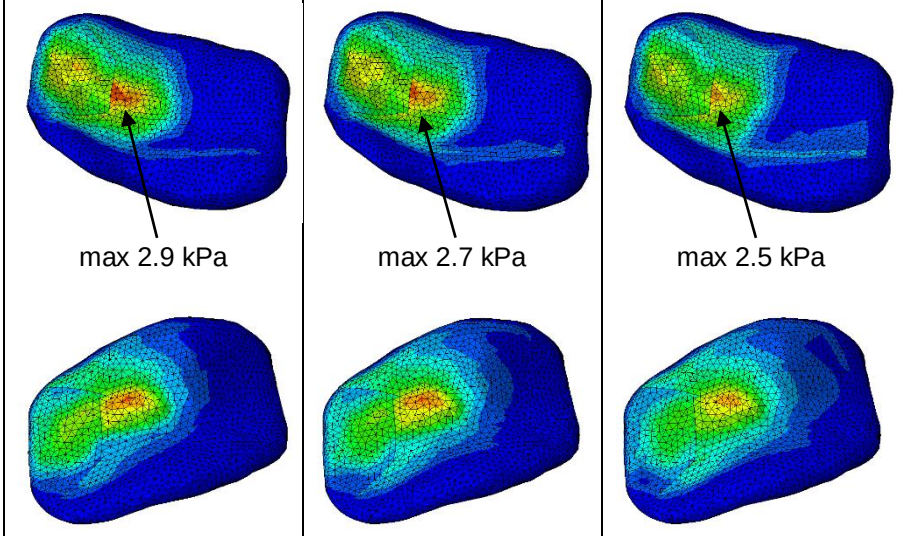		

Figure 7. von Mises stresses in the disc at t = 60 s.

Regarding the stress relaxation ratio at t = 60 s, in these simulations, the value was 54% for the model with uniform disc property. On the other hand, the stress

relaxation ratio was 50% for the model with region-specific disc properties.

3.2 Antero-posterior direction

In Figures 8-10, von Mises stress results of both models in the antero-posterior direction are presented. In these simulations, the largest von Mises stresses on the surface of the TMJ disc were observed when the loading was applied in +5° direction, irrespective of the simulated time.

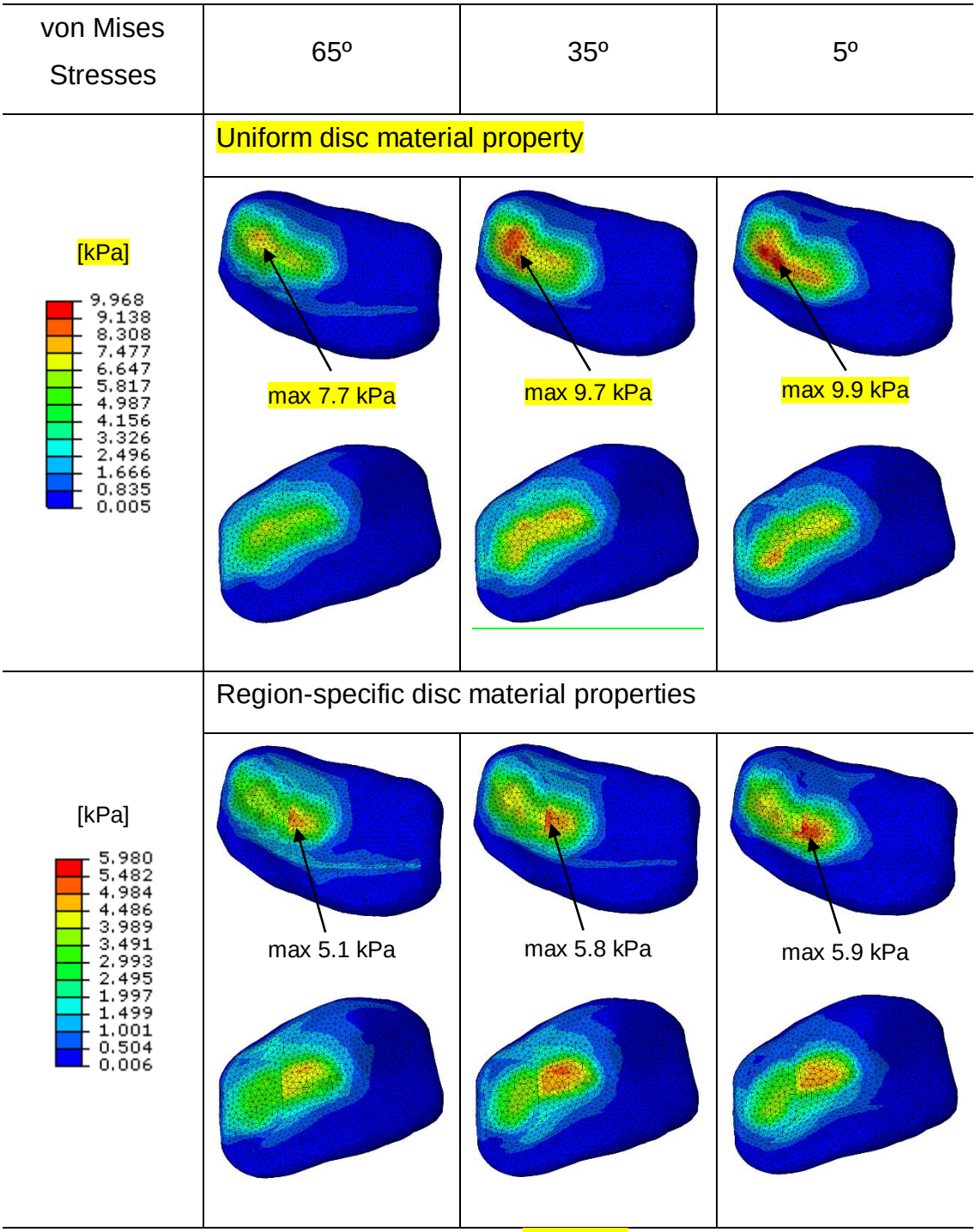

Figure 8. von Mises stresses in the disc at t = 0.1 s.

According to Figure 8, the highest stresses at t = 0.1 s were found in the model with uniform disc property with a value of 9.9 kPa, whereas 5.9 kPa was obtained in the model with region-specific disc properties, which represents a reduction in stress of approximately 40% between models. On the other hand, as seen in Figure 9, the largest stress at t = 1 s was presented in the model with uniform disc property with a value of 7.2 kPa, whereas 4.7 kPa was obtained in the model with region-specific disc properties, which represents a reduction in stress of approximately 35% between models. Moreover, the stresses at t = 60 s were presented in Figure 10. Higher stress values were also obtained for the model with uniform disc property, being the maximum stress values 4.7 kPa for the model with uniform disc property and 3.2 kPa for the model with region-specific disc properties, which represents a reduction in stress of approximately 32% between models.

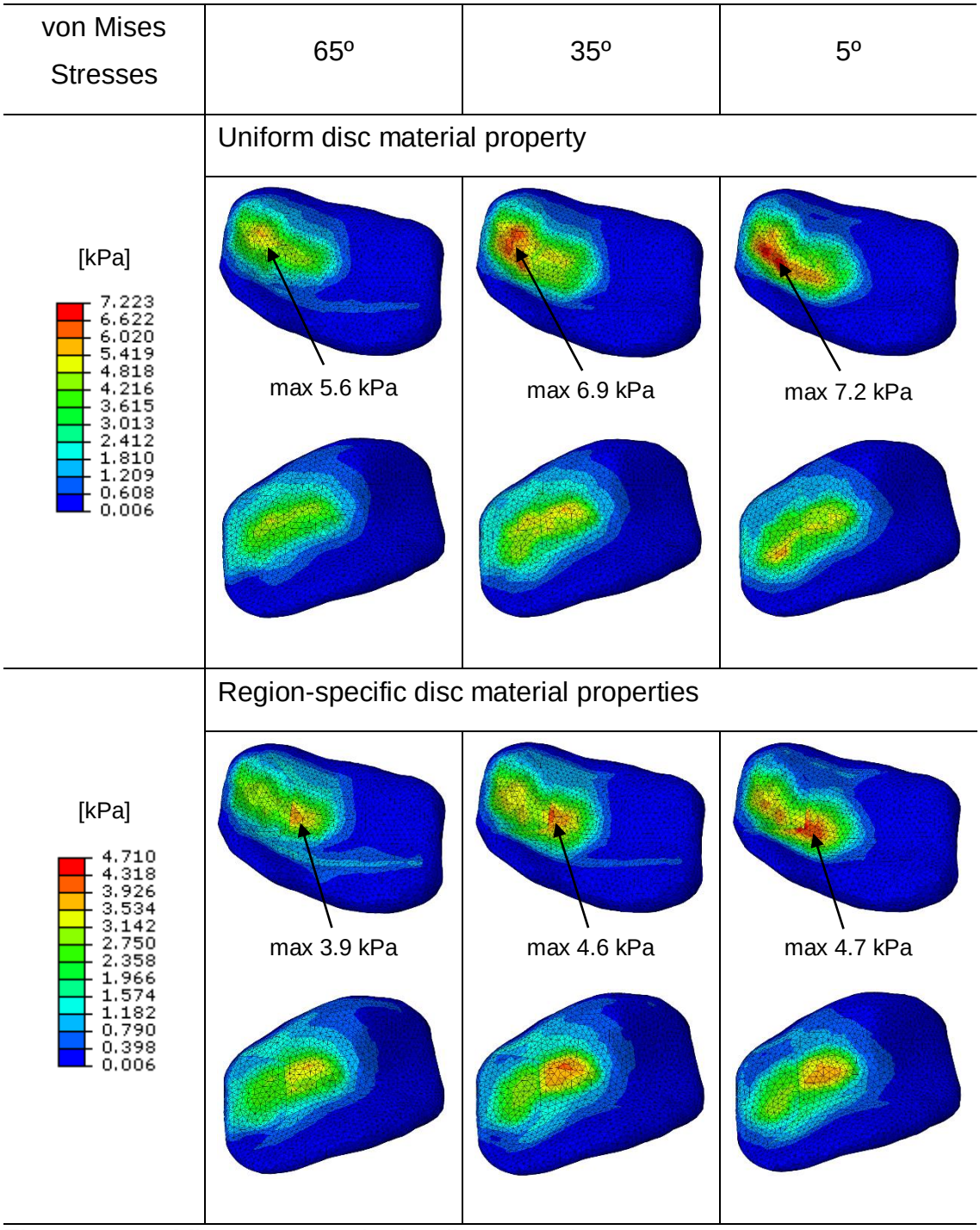

Figure 9. von Mises stresses in the disc at t = 1 s.

Concerning the stress location, as in the medio-lateral direction, the largest von Mises stresses were located in the lateral region for the model with uniform disc property, whereas in the model with region-dependent material properties the largest stresses were located in the central region. Moreover, the influence of the variation of the loading angles in the antero-posterior direction was observed at +5 direction, being the largest stresses, in both models, closer to the anterior

region, at the three instances of time.

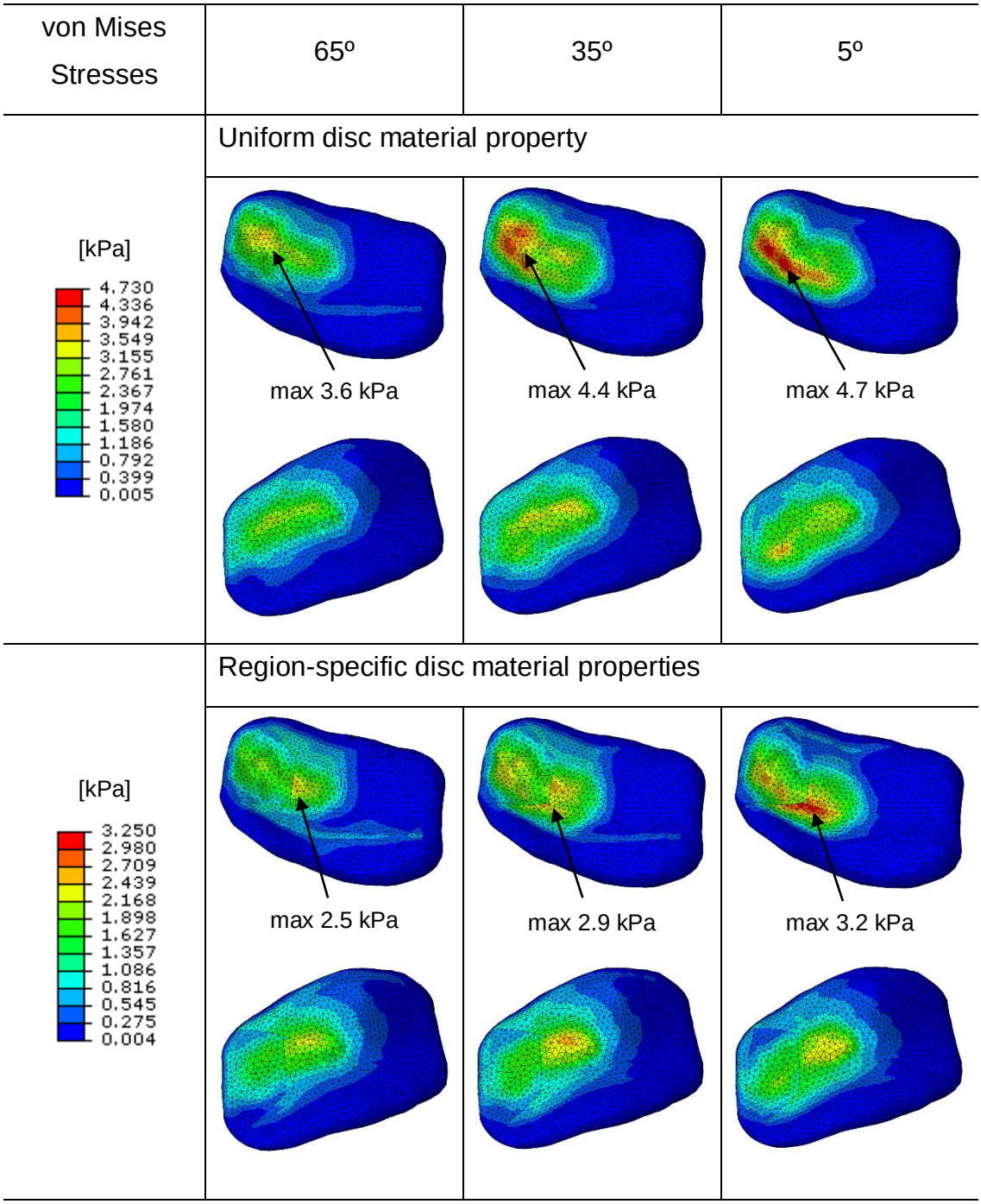

Figure 10. von Mises stresses in the disc at t = 60 s.

Regarding stress relaxation ratio at 60 s, in these simulations a value of 53% was found for the model with uniform disc property. On the other hand, the stress relaxation ratio was 46% for the model with region-specific disc properties. Both were closed to the values found in the medio-lateral direction.

Finally, comparing the effects of the angle variation for the medio-lateral direction and the antero-posterior direction, as it was mentioned, the largest stress was found at -20° for the medio-lateral and at +5° in the antero-posterior. Between both, the larger stress was always found at +5° on the antero-posterior direction.

Discussion

It is well-known that the TMJ disc contributes to control loads exerted by various mandibular movements, and the regulated loads contribute to growth, development and maintenance of the TMJ components (Stegenga et al., 1989). Since the TMJ disc has viscoelastic behavior, it enables stress reduction and distribution in the TMJ components and energy dissipation within the joint tissues (Guerrero Cota et al., 2019; Tanaka et al., 1999; Tanaka & van Eijden, 2003). The compressive moduli mainly depend on the density of the proteoglycans, especially large chondroitin sulfate, while the tensile moduli mainly depend on the amount and orientation of collagen fibers (Detamore & Athanasiou, 2003; Tanaka & van Eijden, 2003). Furthermore, corresponding to the evidence that there is regional dissimilarity in the distribution of proteoglycans and glycosaminoglycans in the TMJ disc (Mizoguchi et al., 1998; Sindelar et al., 2000), the region-specific viscoelastic properties of the TMJ disc have been reported (Barrientos et al., 2019; Chen et al., 2020; Fernández et al., 2013; Guerrero Cota et al., 2019). It has been demonstrated the similarity between the regional distributions of the amount of proteoglycans and the compressive moduli, which supported the biomechanical data of the association between chondroitin sulfate presence and compressive property of the TMJ disc (Fernández et al., 2013; Guerrero Cota et al., 2019). Taken these considerations, the region-specific mechanical properties of the TMJ disc should be used for stress analysis in the TMJ by using a finite element models; however, limited information was available about the effect of region-specific mechanical properties of the TMJ disc on the stress distribution in the TMJ. To our best knowledge, this is the first study in which the difference of stress distribution in the TMJ finite element models with the region-specific moduli and with a representative single modulus was examined.

Data obtained in previous studies using single disc material property (Barrientos et al., 2020) indicated that largest von Mises stresses were located at the lateral region. In addition, larger von Mises stress was found when the loading was applied in the -20° medio-lateral direction. Nonetheless, when the loading was applied in 20° medio-lateral direction, von Mises stress was distributed over a wider area. Moreover, larger von Mises stress was found at t = 0.01 s, In this study, the same observations seen by Barrientos et al. (2020) were found for the

model with single disc material property in the medio-lateral direction, in terms of regional location of the largest von Mises stress, variations on stresses with the loading direction and relaxation ratio. Nonetheless, different values of stress were found due to the differences on the type of contacts and the elements of the disc used. On the other hand, new observations were found for the model with region-specific disc properties, in terms of stresses and its distribution in the different regions.

In the present study differences in stresses were encountered between the model with uniform disc material property and the model with region-specific properties (see Section 3). Even though the differences are dependent on the loading direction and the instance of time, lower values were always obtained in the model with region-specific disc properties. The present results also demonstrated that relatively larger von Mises stresses were present at the anterior, lateral, and central regions of the TMJ disc during prolonged clenching irrespective of time. Previous studies showed stress distributions in the TMJ disc were speculated from anatomical and biochemical findings in the TMJ disc (Scapino et al., 2006; Singh & Detamore, 2009; Tanaka et al., 1994). Anatomical studies with cadavers indicate that marked thinning and perforation of the disc were more frequently found in the anterior, central and lateral regions while the pathological hiascent was often detected in the posterior region, especially at the disc-retrodiscal tissue border (Touré et al., 2005). In addition to that, from the biochemical aspect, the glycosaminoglycan, associated with compressive stresses in the healthy TMJ disc, was distributed greatly in the anterior, central and lateral regions of the TMJ disc but not in the posterior region (Detamore and Athanasiou, 2003; Guerrero Cota et al., 2019; Lin et al., 2018). In both models, the distribution of the compressive stresses in the TMJ disc was similar. Furthermore, Wang et al., (2008), using cadavers, investigated whether the TMJ disc responses to dysfunctional occlusal changes by an increase in thickness, and demonstrated that the TMJ disc has the ability to adapt to alteration of the space between condyle and fossa caused by occlusal changes. This means healthy TMJ disc is likely to show a uniform distribution of stresses on its articular surfaces. Taken these considerations, both models were confirmed to have sufficient physical and biomechanical equivalence to investigate the microcircumstances within the TMJ,

and especially the model with the region-specific disc properties might simulate better the TMJ.

Obviously, the assumptions and simplifications underlying the biomechanical models of the human TMJ should be taken into account when interpreting its predictions (Breedveld, 2004). Furthermore, the results obtained in the present study cannot be immediately transferred to clinical practice without further serious considerations. With respect to the present analysis, the following remarks have to be noticed. First, the material properties of the TMJ disc and cartilage were modelled according to experimental data obtained from porcine TMJ (Barrientos et al., 2020; Fernández et al., 2013), because no reliable material properties for human are available in the previous literatures. While human discs possessed properties distinct from those of the other species, porcine discs are considered to be close to that of humans, suggesting that the pig may be a suitable animal model for TMJ bioengineering efforts (Herring, 2003; Kalpakci et al., 2011). Second, the tensile and shear properties of the TMJ disc were different from the compressive one (Tanaka and van Eijden, 2003). Therefore, the TMJ disc could be regarded as anisotropic materials. In the present study, the anisotropic behaviour of the disc was not taken into account because the disc was subject to compression during prolong clenching irrespective of the loading direction (Barrientos et al., 2020). Nevertheless, further study using an anisotropic disc model should be performed in the future. Third, although biphasic or poroelastic material model is commonly applied to express the material behaviour of articular cartilage (Mow et al., 1984; Prendergast et al., 1996), we adopted the linear viscoelastic generalized Maxwell model to express the biomechanical behaviour of TMJ disc. Allen and Athanasiou (2006) demonstrated that since the TMJ disc contains much less proteoglycans, a viscoelastic model is considered to be more suitable for the TMJ disc. Koolstra et al. (2007) also described that although other mechanical models based upon the poroelastic and biphasic theories could also be fit to these data, these other models may have limitations when modelling the mechanical response of the TMJ disc due to lower concentration of glycosaminoglycans (GAGs). Lower GAG and proteoglycan concentrations are likely to result in a reduced drag between the fluid and solid matrix (Allen and Athanasiou, 2006). For this reason, we selected a viscoelastic model to represent

the TMJ disc as opposed to a poroelastic or a biphasic model. However, in the future, a comparison study between linear and non-linear viscoelastic models should be conducted. Finally, the model geometry was based on MRI data of only one healthy patient. It is true that large variation exists among individuals and there might be an interindividual difference in structure and function of musculoskeletal systems including the TMJ. This implies a large difference in the amount of TMJ stress among the models. Assuming the stress analysis as only one healthy TMJ may be too simplified to for a quantitative analysis of TMJ stress, the present study has to be considered as qualitative.

Conclusions

- The model with uniform disc material property presents higher stresses for the same loading than those obtained using the model with region-specific disc material properties.
- In medio-lateral direction, higher stresses were obtained for the -20º loading direction in both models, whereas lower and more uniform distributed stresses were obtained at 20º. In antero-posterior direction, higher stresses were obtained for the +5º loading direction. Between models, the largest stress was always found at +5º in the antero-posterior direction.
- The highest von Mises stresses were induced in the lateral region for the the model with uniform disc material property. Nevertheless, higher von Mises stresses were also found in the lateral and central region for the model with region-specific disc properties.
- Due to the loading variations at the antero-posterior direction, the highest stresses were found in the lateral region but closer to the anterior region for the model with uniform disc material property. However, the largest stresses were induced in the central and anterior region for the model with region-specific disc properties.
- A clinical implication from these findings is that an early approach to parafunctional habit such as habitual one-sided chewing, bruxism, and clenching would be desirable to reduce excessive stress in the specific region of the disc.

Acknowledgements

The authors would like to express their gratitude to the Spanish Ministry of Economy and Competitiveness for the financial support of the project "Probabilistic prediction of damage and fatigue failure: application to components and structures of polymeric materials" (DPI2016-80389-C22-2-R), as well as to the CajAstur Fellowship-University of Oviedo's 2011 programme.

References

Abe, S., Kawano, F., Kohge, K., Kawaoka, T., Ueda, K., Hattori-Hara, E., Mori, H., Kuroda, S., Tanaka, E., 2013. Stress analysis in human temporomandibular joint affected by anterior disc displacement during prolonged clenching. J. Oral Rehabil. 40, 239–246. https://doi.org/10.1111/joor.12036

Allen, K.D., Athanasiou, K.A., 2006. Viscoelastic characterization of the porcine temporomandibular joint disc under unconfined compression. J. Biomech. 39, 312–322. https://doi.org/10.1016/j.jbiomech.2004.11.012

Barrientos, E., Pelayo, F., Noriega, Á., Lamela, M.J., Fernández-Canteli, A., Tanaka, E., 2019. Optimal discrete-time Prony series fitting method for viscoelastic materials. Mech. Time-Dependent Mater. 23, 193–206. https://doi.org/10.1007/s11043-018-9394-z

Barrientos, E., Pelayo, F., Tanaka, E., Lamela-Rey, M.J., Fernández-Canteli, A., 2016. Dynamic and stress relaxation properties of the whole porcine temporomandibular joint disc under compression. J. Mech. Behav. Biomed. Mater. 57, 109–115. https://doi.org/10.1016/j.jmbbm.2015.12.003

Barrientos, E., Pelayo, F., Tanaka, E., Lamela-Rey, M.J., Fernández-Canteli, A., de Vicente, J.C., 2020. Effects of loading direction in prolonged clenching on stress distribution in the temporomandibular joint. J. Mech. Behav. Biomed. Mater. 112. https://doi.org/10.1016/j.jmbbm.2020.104029

Beek, M., Koolstra, J.H., van Ruijven, L.J., van Eijden, T.M.G.J., 2000. Three-dimensional finite element analysis of the human temporomandibular joint disc. J. Biomech. 33, 307–316. https://doi.org/10.1016/S0021-9290(99)00168-2

Breedveld, F.C., 2004. Osteoarthritis--the impact of a serious disease. Rheumatology 43, 4i – 8. https://doi.org/10.1093/rheumatology/keh102

Chen, D., Wu, J.Y., Kennedy, K.M., Yeager, K., Bernhard, J.C., Ng, J.J., Zimmerman, B.K., Robinson, S., Durney, K.M., Shaeffer, C., Vila, O.F., Takawira, C., Gimble, J.M., Guo, X.E., Ateshian, G.A., Lopez, M.J., Eisig, S.B., Vunjak-Novakovic, G., 2020. Tissue engineered autologous cartilage-bone grafts for temporomandibular joint regeneration. Sci. Transl. Med. 12, eabb6683. https://doi.org/10.1126/scitranslmed.abb6683

Chen, T., 2000. Determining a Prony Series for a Viscoelastic Material From Time Strain Data Varying.

del Pozo, R., Tanaka, E., Tanaka, M., Okazaki, M., Tanne, K., 2002. The regional difference of viscoelastic property of bovine temporomandibular joint disc in compressive stress-relaxation. Med. Eng. Phys. 24, 165–171. https://doi.org/10.1016/S1350-4533(01)00127-8

Detamore, M.S., Athanasiou, K.A., 2003. Structure and function of the temporomandibular joint disc: Implications for tissue engineering. J. Oral Maxillofac. Surg. 61, 494–506. https://doi.org/10.1053/joms.2003.50096

Detamore, M.S., Orfanos, J.G., Almarza, A.J., French, M.M., Wong, M.E., Athanasiou, K.A., 2005. Quantitative analysis and comparative regional investigation of the extracellular matrix of the porcine temporomandibular joint disc. Matrix Biol. 24, 45–57. https://doi.org/10.1016/j.matbio.2004.11.006

Donzelli, P.S., Gallo, L.M., Spilker, R.L., Palla, S., 2004. Biphasic finite element simulation of the TMJ disc from in vivo kinematic and geometric measurements. J. Biomech. 37, 1787–1791. https://doi.org/10.1016/j.jbiomech.2004.01.029

Emri, I., von Bernstorff, B.S., Cvelbar, R., Nikonov, A., 2005. Re-examination of the approximate methods for interconversion between frequency- and time-dependent material functions. J. Nonnewton. Fluid Mech. 129, 75–84. https://doi.org/10.1016/j.jnnfm.2005.05.008

Fernández, P., Jesús Lamela, M., Ramos, A., Fernández-Canteli, A., Tanaka, E., 2013. The region-dependent dynamic properties of porcine temporomandibular joint disc under unconfined compression. J. Biomech. 46, 845–848. https://doi.org/10.1016/j.jbiomech.2012.11.035

Guerrero Cota, J.M., Leale, D.M., Arzi, B., Cissell, D.D., 2019. Regional and disease-related differences in properties of the equine temporomandibular joint disc. J. Biomech. 82, 54–61. https://doi.org/10.1016/j.jbiomech.2018.10.017

Hattori-Hara, E., Mitsui, S.N., Mori, H., Arafurue, K., Kawaoka, T., Ueda, K., Yasue, A., Kuroda, S., Koolstra, J.H., Tanaka, E., 2014. The influence of unilateral disc displacement on stress in the contralateral joint with a normally positioned disc in a human temporomandibular joint: An analytic approach using the finite element method. J. Cranio-Maxillofacial Surg. 42, 2018–2024. https://doi.org/10.1016/j.jcms.2014.09.008

Herring, S.W., 2003. TMJ anatomy and animal models. J. Musculoskelet. Neuronal Interact. 3, 391–4; discussion 406-7.

Hirose, M., Tanaka, E., Tanaka, M., Fujita, R., Kuroda, Y., Yamano, E., van Eijden, T.M.G.J., Tanne, K., 2006. Three-dimensional finite-element model of the human temporomandibular joint disc during prolonged clenching. Eur. J. Oral Sci. 114, 441–448. https://doi.org/10.1111/j.1600-0722.2006.00389.x

Kalpakci, K.N., Willard, V.P., Wong, M.E., Athanasiou, K.A., 2011. An Interspecies Comparison of the Temporomandibular Joint Disc. J. Dent. Res. 90, 193–198. https://doi.org/10.1177/0022034510381501

Koolstra, J.H., Tanaka, E., Van Eijden, T.M.G.J., 2007. Viscoelastic material model for the temporomandibular joint disc derived from dynamic shear tests or strain-relaxation tests. J. Biomech. 40, 2330–2334. https://doi.org/10.1016/j.jbiomech.2006.10.019

Koolstra, J.H., van Eijden, T.M.G.J., 2005. Combined finite-element and rigid-body analysis of human jaw joint dynamics. J. Biomech. 38, 2431–2439. https://doi.org/10.1016/j.jbiomech.2004.10.014

Lin, A.W., Vapniarsky, N., Cissell, D.D., Verstraete, F.J.M., Lin, C.H., Hatcher, D.C., Arzi, B., 2018. The Temporomandibular Joint of the Domestic Dog (Canis lupus familiaris) in Health and Disease. J. Comp. Pathol. 161, 55–67. https://doi.org/10.1016/j.jcpa.2018.05.001

Mizoguchi, I., Scott, P.G., Dodd, C.M., Rahemtulla, F., Sasano, Y., Kuwabara, M., Satoh, S., Saitoh, S., Hatakeyama, Y., Kagayama, M., Mitani, H., 1998. An immunohistochemical study of the localization of biglycan, decorin and large chondroitin-sulphate proteoglycan in adult rat temporomandibular joint disc. Arch. Oral Biol. 43, 889–898. https://doi.org/10.1016/S0003-9969(98)00038-7

Mow, V.C., Holmes, M.H., Michael Lai, W., 1984. Fluid transport and mechanical properties of articular cartilage: A review. J. Biomech. 17, 377–394. https://doi.org/10.1016/0021-9290(84)90031-9

Nakano, T., Scott, P.G., 1989. A quantitative chemical study of glycosaminoglycans in the articular disc of the bovine temporomandibular joint. Arch. Oral Biol. 34, 749–757. https://doi.org/10.1016/0003-9969(89)90082-4

Ninomiya, K., Ferry, J.D., 1959. Some approximate equations useful in the

phenomenological treatment of linear viscoelastic data. J. Colloid Sci. 14, 36–48. https://doi.org/10.1016/0095-8522(59)90067-4

Pérez del Palomar, A., Doblaré, M., 2006. On the numerical simulation of the mechanical behaviour of articular cartilage. Int. J. Numer. Methods Eng. 67, 1244–1271. https://doi.org/10.1002/nme.1638

Prendergast, P.J., van Driel, W.D., Kuiper, J.-H., 1996. A Comparison of Finite Element Codes for the Solution of Biphasic Poroelastic Problems. Proc. Inst. Mech. Eng. Part H J. Eng. Med. 210, 131–136. https://doi.org/10.1243/PIME_PROC_1996_210_402_02

Scapino, R.P., Canham, P.B., Finlay, H.M., Mills, D.K., 1996. The behaviour of collagen fibres in stress relaxation and stress distribution in the jawjoint disc of rabbits. Arch. Oral Biol. 41, 1039–1052. https://doi.org/10.1016/S0003-9969(96)00079-9

Scapino, R.P., Obrez, A., Greising, D., 2006. Organization and Function of the Collagen Fiber System in the Human Temporomandibular Joint Disk and Its Attachments. Cells Tissues Organs 182, 201–225. https://doi.org/10.1159/000093969

Simulia, 2016. Defining tied contact in Abaqus/Standard [WWW Document]. Abaqus/CAE User's Guid. URL https://abaqus-docs.mit.edu/2017/English/SIMACAEITNRefMap/simaitn-c-tiedcontact.htm (accessed 1.15.21).

Sindelar, B.J., Evanko, S.P., Alonzo, T., Herring, S.W., Wight, T., 2000. Effects of Intraoral Splint Wear on Proteoglycans in the Temporomandibular Joint Disc. Arch. Biochem. Biophys. 379, 64–70. https://doi.org/10.1006/abbi.2000.1855

Singh, M., Detamore, M.S., 2009. Biomechanical properties of the mandibular condylar cartilage and their relevance to the TMJ disc. J. Biomech. 42, 405–417. https://doi.org/10.1016/j.jbiomech.2008.12.012

Stegenga, B., De Bont, L.G.M., Boering, G., 1989. A proposed classification of temporomandibular disorders based on synovial joint pathology. Cranio - J. Craniomandib. Pract. 7, 107–118. https://doi.org/10.1080/08869634.1989.11678273

Tanaka, E., del Pozo, R., Tanaka, M., Asai, D., Hirose, M., Iwabe, T., Tanne, K., 2004. Three-dimensional finite element analysis of human

temporomandibular joint with and without disc displacement during jaw opening. Med. Eng. Phys. 26, 503–511. https://doi.org/10.1016/j.medengphy.2004.03.001

Tanaka, E., Hirose, M., Koolstra, J.H., van Eijden, T.M.G.J., Iwabuchi, Y., Fujita, R., Tanaka, M., Tanne, K., 2008. Modeling of the Effect of Friction in the Temporomandibular Joint on Displacement of Its Disc During Prolonged Clenching. J. Oral Maxillofac. Surg. 66, 462–468. https://doi.org/10.1016/j.joms.2007.06.640

Tanaka, E., Hirose, M., Yamano, E., Dalla-Bona, D.A., Fujita, R., Tanaka, M., van Eijden, T., Tanne, K., 2006. Age-associated changes in viscoelastic properties of the bovine temporomandibular joint disc. Eur. J. Oral Sci. 114, 70–73. https://doi.org/10.1111/j.1600-0722.2006.00265.x

Tanaka, E., Pelayo, F., Kim, N., Lamela, M.J., Kawai, N., Fernández-Canteli, A., 2014. Stress relaxation behaviors of articular cartilages in porcine temporomandibular joint. J. Biomech. 47, 1582–1587. https://doi.org/10.1016/j.jbiomech.2014.03.007

Tanaka, E., Tanaka, M., Miyawaki, Y., Tanne, K., 1999. Viscoelastic properties of canine temporomandibular joint disc in compressive load-relaxation. Arch. Oral Biol. 44, 1021–1026. https://doi.org/10.1016/S0003-9969(99)00097-7

Tanaka, E., Tanne, K., Sakuda, M., 1994. A three-dimensional finite element model of the mandible including the TMJ and its application to stress analysis in the TMJ during clenching. Med. Eng. Phys. 16, 316–322. https://doi.org/10.1016/1350-4533(94)90058-2

Tanaka, E., van Eijden, T., 2003. Biomechanical Behavior of the Temporomandibular Joint Disc. Crit. Rev. Oral Biol. Med. 14, 138–150. https://doi.org/10.1177/154411130301400207

Touré, G., Duboucher, C., Vacher, C., 2005. Anatomical modifications of the temporomandibular joint during ageing. Surg. Radiol. Anat. 27, 51–55. https://doi.org/10.1007/s00276-004-0289-0

Tschoegl, N.W., 2012. The Phenomenological Theory of Linear Viscoelastic Behavior: An Introduction [WWW Document]. Springer, Berlin. URL https://books.google.es/books?hl=es&lr=&id=7Kf7CAAAQBAJ&oi=fnd&pg=PR7&dq=Tschoegl,+N.W.:+The+Phenomenological+Theory+of+Linear+Viscoelastic+Behavior:+An+Introduction.+Springer,+Berlin+(2012)&ots=aZc9e

Ae0Sj&sig=-Ea3cVeFEq7w4R-MdtT2roSjA7w#v=onepage&q=Tscho (accessed 1.11.21).

Wang, M.-Q., He, J.-J., Li, G., Widmalm, S.E., 2008. The effect of physiological nonbalanced occlusion on the thickness of the temporomandibular joint disc: A pilot autopsy study. J. Prosthet. Dent. 99, 148–152. https://doi.org/10.1016/S0022-3913(08)60031-1

Appendix A

Tables with relaxation modulus obtained from Ninomiya-Ferry Conversion (Ninomiya and Ferry, 1959) from Complex moduli (Fernández et al., 2013).

Note: $E(t)$ is the mean and E_{max} and E_{min} are the maximum and minimum limits for each time interval.

Table A1: Anterior relaxation modulus

Time [s]	E [Pa]	E_{max} [Pa]	E_{min} [Pa]
0.1	65584	81503	49665
0.26827	58906	73057	44754
0.71969	52978	65583	40373
1.9307	48033	59246	36820
5.1795	42943	53190	32696
13.895	39205	48178	30231
37.276	34171	41936	26406
100	30437	37433	23442

Table A2. Central relaxation modulus

Time [s]	E [Pa]	E_{max} [Pa]	E_{min} [Pa]
0.1	63799	73665	53933
0.26827	56287	64859	47715
0.71969	50250	58220	42280
1.9307	45284	52232	38336
5.1795	40501	46988	34014
13.895	36652	42415	30888
37.276	31228	36415	26041
100	27178	32033	22322

Table A3. Lateral relaxation modulus

Time [s]	E [Pa]	E_{max} [Pa]	E_{min} [Pa]
0.1	46379	49502	43284
0.26827	40583	44745	36993
0.71969	37601	41777	32982
1.9307	33727	38478	29030
5.1795	31734	36684	25407
13.895	27541	31939	23738
37.276	22882	27203	19529
100	19756	24206	15961

Table A4. Medial relaxation modulus

Time [s]	E [Pa]	E_{max} [Pa]	E_{min} [Pa]
0.1	56108	64386	47830
0.26827	50254	57463	43045
0.71969	45290	51797	38783
1.9307	40828	46360	35297
5.1795	36643	41605	31681
13.895	33285	37875	28694
37.276	28635	32836	24433
100	25184	29120	21247

Table A5. Posterior relaxation modulus

Time [s]	E [Pa]	E_{max} [Pa]	E_{min} [Pa]
0.1	68567	87481	49653
0.26827	61336	77749	45143
0.71969	55212	70050	40202
1.9307	49788	63081	36538
5.1795	44968	56208	33206
13.895	40563	50687	30619
37.276	35482	43261	26882
100	31934	37776	24092

Tables with linear viscoelastic models for each region

Table A6. Posterior region Prony coefficients

Poisson ratio, ν	0.4
Young Modulus, E_0 [MPa]	0.0655
Prony terms	
e_1	0.2621
τ_1	0.6795
e_2	0.1484
τ_2	9.6169
e_3	0.1589
τ_3	64.1328

Table A7. Anterior region Prony coefficients

Poisson ratio, ν	0.4
Young Modulus, E_0 [MPa]	0.0637
Prony terms	
e_1	0.2243
τ_1	0.5059
e_2	0.1152

τ_2	2.5165
e_3	0.2444
τ_3	31.1899

Table A8. Central region Prony coefficients

Poisson ratio, ν	0.4
Young Modulus, E_0 [MPa]	0.0463
Prony terms	
e_1	0.2458
τ_1	0.5344
e_2	0.1934
τ_2	14.3452
e_3	0.1551
τ_3	49.2614

Table A9. Lateral region Prony coefficients

Poisson ratio, ν	0.4
Young Modulus, E_0 [MPa]	0.0561
Prony terms	
e_1	0.2039
τ_1	0.5387
e_2	0.1182
τ_2	2.4615
e_3	0.2384
τ_3	30.9592

Table A10. Medial region Prony coefficients

Poisson ratio, ν	0.4
Young Modulus, E_0 [MPa]	0.0685
Prony terms	
e_1	0.2291
τ_1	0.5702
e_2	0.1074

τ_2	3.6769
e_3	0.2056
τ_3	30.4911

1